The Influence of Stochastic Parameters on Calcium Waves in a Heart Cell

Matthew W. Brewster
Department of Mathematics and Statistics, University of Maryland, Baltimore County

Abstract

Calcium is a critical component in many cellular functions. It serves many important functions such as signal transduction, contraction of muscles, enzyme function, and maintaining potential difference across excitable membranes. In this study we examine calcium waves in a heart cell and how they diffuse. Calcium sparks are intracellular release events which are important in converting electrical stimuli into mechanical responses. We investigate the effects of a stochastic spatially uniform flux density term as well as of a stochastic spatially varying flux density term. We hypothesize that having a stochastic flux density term is more physiologically accurate. We use an array of statistical techniques as well as parallel computing to facilitate the large number of simulation runs.

1 INTRODUCTION

Calcium is a critical component in many cellular functions. It serves many important functions such as signal transduction, contraction of muscles, enzyme function, and maintaining potential difference across excitable membranes. Calcium in mammals is stored in their bones and the calcium ions are released from the bone under controlled conditions and are then transported through the blood stream. In this study we examine calcium waves in heart cells and how they diffuse. Calcium sparks are intracellular Ca^{2+} release events which are important in converting electrical stimuli into mechanical responses. In cardiac muscle cells Ca^{2+} sparks arise from the activation of ryanodine receptors which causes Ca^{2+} from the sarcoplasmic reticulum. The calcium ions generated by the spark create waves which diffuse throughout the cell and can replicated.

The existing model for calcium flow is given by a system of coupled, time-dependent advection-reaction-diffusion equations

$$\frac{\partial u^{(i)}}{\partial t} - \nabla \cdot \left(D^{(i)} \nabla u^{(i)}\right) + \beta^{(i)} \cdot \nabla u^{(i)} = r^{(i)} + \left(- J_{\text{pump}} + J_{\text{leak}} + J_{\text{SR}}\right)\, \delta_{i1} \tag{1.1}$$

for concentrations $u^{(i)}(\mathbf{x}, t)$ of the $n_s = 3$ chemical species $i = 1, \ldots, n_s$ as functions of space $\mathbf{x} \in \Omega \subset \mathbb{R}^3$ and time $0 \le t \le t_{\text{fin}}$ [6]. This model is coupled with no flow boundary conditions in the cell wall, and the concentrations at the initial time are set at basal levels. The second term models diffusion with diffusivity $D^{(i)} \in \mathbb{R}^{3\times 3}$. Next, the third term is the advection term with velocity $\beta^{(i)} \in \mathbb{R}^3$. $r^{(i)}$ are the reaction terms which are nonlinear functions of different species and couple the three equations. Terms belonging only to the equation for calcium species $i = 1$ are multiplied with the Kronecker delta function $\delta_{i1} = 1$ if $i = 1$ and $\delta_{i1} = 0$ otherwise.

- **Uniform CRU Flux Density: (UCFD)** The key term of the model is the

$$J_{\text{SR}}(u^{(1)}, x, t) = \sum_{\hat{x}\ \in\ \Omega_{\text{s}}} g\ \text{S}_{\hat{x}}(u^{(1)}, t)\ \delta(x - \hat{x}) \tag{1.2}$$

  which describes the release of calcium for all calcium release units (CRUs) in the set of CRUs Ω_s [2,4]. The release of calcium at each CRU is modeled as a point source on the spatial scale of the cell and is represented mathematically as a Dirac delta distribution $\delta(x-\hat{x})$ for a CRU located at $\hat{x}$. Recall from the definition of the Dirac delta distribution that (i) $\delta(x - \hat{x}) = 0$ when $x \neq \hat{x}$ and (ii) $\int_\Omega \psi(x)\delta(x - \hat{x})dx = \psi(\hat{x})$ for any continuous function $\psi(x)$. We get the amount of calcium injected into the cell at one point $\hat{x}$ is given by the flux density g, that is,

$\int_\Omega g\delta(x-\hat{x})dx = g$ by the definition of delta distribution. Thus g gives the amount of calcium released into the cell in 1 ms. The effect of a CRU switching in and off is incorporated by the indicator function $\mathrm{S}_{\hat{x}}$, where $\mathrm{S}_{\hat{x}} = 1$ when the CRU is turned on and $\mathrm{S}_{\hat{x}} = 0$ when CRU is turned off. In the original model $g \equiv const.$ was kept constant for all CRUs and for all time.

- **Stochastic Uniform CRU Flux Density (SUCFD):** First, we investigate the effects of introducing a new J_{SR} given by

$$J_{\mathrm{SR}}(u^{(1)}, \mathbf{x}, t) = \sum_{\hat{x}\ \in\ \Omega_{\mathrm{s}}} g\ \mathrm{S}_{\hat{\mathbf{x}}}(u^{(1)}, t)\ \delta(\mathbf{x} - \hat{x}), \tag{1.3}$$

  in which the g term such that $g \in N(\mu_g, \sigma_g)$ for all CRUs while keeping all other parameters constant.

- **Stochastic Independent CRU Flux Density (SICFD):** Next, we investigate the effects of introducing another J_{SR} term which utilizes stochastic g term at any CRU, $g_{\hat{\mathbf{x}}} \in N(\mu_g, \sigma_g)\ \forall\ \hat{\mathbf{x}} \in \Omega_s$, which will vary the amount of calcium injected into the cell at each CRU. Therefore, $g_{\hat{\mathbf{x}}}$ varies in space, but is constant in time. The new J_{SR} term is given by

$$J_{\mathrm{SR}}(u^{(1)}, x, t) = \sum_{\hat{x}\ \in\ \Omega_{\mathrm{s}}} g_{\hat{x}}\mathrm{S}_{\hat{x}}(u^{(1)}, t)\ \delta(x - \hat{x}). \tag{1.4}$$

By experimenting with stochastic g values and $g_{\hat{x}}$ values we hope to create a more physiologically accurate model and better understand the the effects of the flux density on the model. To examine the effects of stochastic g and $g_{\hat{x}}$ values we will look at the correlation between them and the total μM of calcium over the entire domain Ω, given by $I^{(1)} = \int_\Omega u^{(1)}dx$. [1, 3, 5].

2 THE MODEL

The model for calcium flow in a heart cell given by (1.1) consists of $n_s = 3$ equations, where $(i = 1)$ represents calcium, $(i = 2)$ represents an endogenous calcium buffer, and $(i = 3)$ represents a fluorescent indicator dye. We neglect the advective effects by setting $\beta^{(i)} \equiv 0$ for $i = 1, 2, 3$. The reaction terms $r^{(i)}$ are nonlinear functions of the different species and couple the three equations. The reversible binding and unbinding of the indicator and buffer species are described by the the reaction model

$$\mathrm{C} + \mathrm{F} \rightleftharpoons \mathrm{G}$$
$$\mathrm{C} + \mathrm{B} \rightleftharpoons \mathrm{H}$$

where C has concentration $u^{(1)}$, F has concentration $u^{(2)}$, and B has concentration $u^{(3)}$. represent the calcium ions, the fluorescent calcium indicator, and endogenous buffer respectively. We let G have concentration $u^{(4)}$ and H have concentration $u^{(5)}$ represent the F and B bound to calcium. The reactions rates for these species are given by

$$R^{(2)} = -k_2^+ u^{(1)}u^{(2)} + k_2^- u^{(4)},$$
$$R^{(3)} = -k_3^+ u^{(1)}u^{(3)} + k_3^- u^{(5)}.$$

The total of bound and unbound indicator and buffer species is conserved, that is, $u^{(2)} + u^{(4)} = \overline{u}_2$ and $u^{(3)} + u^{(5)} = \overline{u}_3$ can be used to eliminate $u^{(4)}$ and $u^{(5)}$ from the reaction rates [4]. Therefore, we get the reaction terms:

$$r^{(i)}(u^{(1)}, \ldots, u^{(n_s)}) := \begin{cases} \displaystyle\sum_{j=2}^{n_s} R^{(j)}(u^{(1)}, u^{(j)}), & \text{for } i = 1, \\ R^{(i)}(u^{(1)}, u^{(i)}), & \text{for } i = 2, \ldots, n_s. \end{cases}$$

with reaction rates

$$R^{(i)} = -k_i^+ u^{(1)} u^{(i)} + k_i^- \left(\overline{u}_i - u^{(i)} \right) \qquad \text{for } i = 2, \ldots, n_s.$$

One to the terms of the calcium equation with $i = 1$ are multiplied with Kroneker delta function δ_{i1}. These are the nonlinear drain term J_{pump}, the constant balance term J_{leak}, and the calcium release term J_{SR} [4].

The J_{pump} term is given by the equation

$$J_{\text{pump}}(u^{(1)}) = \frac{V_{pump} (u^{(1)})^{n_{pump}}}{(K_{pump})^{n_{pump}} + (u^{(1)})^{n_{pump}}}.$$

$J_{\text{leak}} = J_{\text{pump}}(0.1) \equiv const.$ for the calcium concentration at basal level 0.1 μM. A complete list of model's parameter values is given in Table 1.

Table 1: Table of parameters for the calcium wave model.

Parameter	Description	Values/Units
Ω	Rectangular domain in μm	$(-6.4, 6.4) \times (-6.4, 6.4) \times (-32.0, 32.0)$
$D^{(1)}$	Calcium diffusion coefficent	$\text{diag}(0.15, 0.15, 0.30)$ μm^2/ ms
$D^{(2)}$	Mobile buffer diffusion coefficient	$\text{diag}(0.01, 0.01, 0.02)$ μm^2/ ms
$D^{(3)}$	Stationary buffer diffusion coefficient	$\text{diag}(0.00, 0.00, 0.00)$ μm^2/ ms
$\beta^{(i)}$	Advection velocity term	$(0, 0, 0)^T$
$u_{\text{ini}}^{(1)}$	Initial calcium concentration	0.1 μM
$u_{\text{ini}}^{(2)}$	Initial mobile buffer concentration	45.9184 μM
$u_{\text{ini}}^{(3)}$	Initial stationary buffer concentration	111.8182 μM
Δx_s	CRU spacing in x direction	0.8 μm
Δy_s	CRU spacing in y direction	0.8 μm
Δz_s	CRU spacing in z direction	0.2 μm
g	Flux density distribution	M μm^3
μ_g	Flux density mean	75 M μm^3
σ_g	Flux density standard deviation	25 M μm^3
F	Faraday constant	96,485.3 C/M
P_{max}	Maximum probability rate	0.3 ms
K_{prob}	Probability sensitivity	0.2 μM
n_{prob}	Probability Hill coefficient	4.0
Δt_s	CRU time step	1.0 ms
t_{open}	CRU opening time	5.0 ms
t_{closed}	CRU refractory period	100 ms
k_2^+	Forward reaction rate	0.08 μM ms
k_2^-	Backward reaction rate	0.09 / ms
$\bar{u}_2$	Total of bound and unbound indicator	50.0 μM
k_3^+	Forward reaction rate	0.10 μM ms
k_3^-	Backward reaction rate	0.10 / ms
$\bar{u}_3$	Total bound and unbound buffer	123.0 μM
v_{pump}	Maximum pump strength	4.0 μM ms
k_{pump}	Pump sensitivity	0.184 μM
n_{pump}	Pump Hill coefficient	4
J_{leak}	Leak term	0.320968365152510 μM / ms

3 METHODS

3.1 Simulation Tools For Calcium Waves

In order to simulate the calcium spark model memory efficient numerical methods are implemented. The uniform rectangular CRU lattice is used to create a regular numerical mesh. The model uses constant diffusion coeffcients. We use the finite volume method for spatial discretization. The parameters to control the timestep selection in the time stepping NDFk method are $\tau_{rel}^{ode} = 10^{-6}$ and $\tau_{abs}^{ode} = 10^{-8}$ and the tolerance for the Newton solver is $\tau^{newt} = 10^{-4}$. The Krylov subspace method used to solve the system of linear equations is BiCGSTAB with tolerance $\tau^{lin} = 10^{-2}$.

The C code used to perform the parallel computations uses MPI for parallel communications. The computations for this study are preformed on the cluster tara using C/MPI under the Linux operating system RedHat Enterprise Linux 5 on multiple nodes. This cluster has a total of 86 nodes. Each node features two quad-core Intel Nehalem X5550 processors (2.66 GHz, 8 MB cache) with 24 GB of memory. To distribute the vector of unknowns among p processes, we split the mesh in the z-direction and distribute the unknowns into p subdomains for p parallel processes. For more specifics refer on how this problem was parallelized refer to [6].

3.2 Stochastic Parameter Study

In order to understand the effects of SUCFD and SICFD on the model we must repeatedly sample g and $g_{\hat{x}}$ from a normal distribution given by $N(\sigma, \mu)$ by running the code M number to times. For both g and $g_{\hat{x}}$ we have chosen to use a normal distribution with $\sigma = 75$ and $\mu = 25$.

After M runs have been performed, we determine the linear correlation between g and the total μM of calcium. To do this we use the Pearson product-moment correlation coefficient to measure the linear correlation between the two variables. To calculate this coefficient we use the formula

$$r = \frac{\Sigma_{i=1}^{M}(X_i - \bar{X})(Y_i - \bar{Y})}{\sqrt{\Sigma_{i=1}^{M}(X_i - \bar{X})^2}\sqrt{\Sigma_{i=1}^{M}(Y_i - \bar{Y})^2}}, \tag{3.1}$$

where X_i and Y_i are vectors of length M and $\bar{X}$ and $\bar{Y}$ are the average values of the elements of the vectors. r will have a value between -1 and 1. If $r = 0$ then the two variables exhibit no correlation. If $r < 0$ then the variable have a negative correlation which means that as one variable increases the other decreases. If $r > 0$ then the variables have a positive correlation and as one variable increases the other variable increases. The closer r is to 1 or -1 the more the variables are correlated.

To automate the running of the SUCFD case a series of three bash scripts. The first bash script automates the creation of M directories each with a dynamically generated input file such that g is sampled from a normal distribution $N(\mu_g, \sigma_g)$. Then another bash script submits and runs instance of the spark code and a dynamically generated spark file and stores the data for each run in each directory. Then a post-processing script stores the run number, associated g, and the value of the calcium integral and generates plots with Matlab. Further post-processing is done with another series of Matlab scripts to create animations of the data. A similar method will be used for the SICFD case except that an array of g values will be created for each CRU for M runs.

4 RESULTS

4.1 Visualization of Simulations of Calcium Induced Calcium Flow

We solve the model of calcium induced calcium flow given by a system of coupled, time-dependent advection-reaction-diffusion equations (1.1), where the calcium injection is modeled by (1.2) with a constant uniform CRU flux density. The parameters are given in Table 1. Currently, there are several different ways of analyzing the behavior of the calcium simulations. To illustrate the different visualization tool we plot the simulations with g held constant. We first show three ways to visualize the simulation when $g = 110$ constant uniformly at all CRUs. In this case, we have several waves self initiate and propagate throughout the cell. The first plotting method is called CRU Plot, shown in Figure 1. The plots in this figure show which CRUs are open at each timestep during the simulation. We see that at $t = 100$ a few CRUs are open, the wave mostly spreads along x and y dimensions at this point. Later on we see that the CRUs have begun to open on both sides of the cell and spread across it. During our simulation of 1000 ms, several waves have been generated and run across the cell. The second plotting method is called Isosurface Plot, shown in Figure 2. The plots in the figure show the same time steps as in the CRU plots, but on the calcium concentration. The Isosurface Plots give us a 3-dimensional representation how the calcium diffuses through the cell based on the concentration of calcium species u_1. An isosurface plot shows the surface in three dimensions, on which the concentration of equals the critical value $u_{crit} = 65\mu$M. Inside the surface, the concentration is higher than u_{crit}, while outside the plotted area the concentration is lower than u_{crit}. Where the surface with $u_1 = u_{crit}$ touches the boundary of the domain, the concentration may be higher than u_{crit}, and this is indicates by the color palette increasing from blue over yellow to red. Again, we see that when $t = 100$ in Figure 2 there is a small amount of calcium in the cell. As time advances, we see that the amount of calcium in the cell increases and diffuses throughout the cell. The third plotting method is called Confocal Image Plot, shown in Figure 3. The confocal images are meant to replicate what scientists see in the laboratory experiments using florescent dye to bind to the calcium in the heart cell. The lighter of green shades indicate higher calcium concentrations, while the darker green shades indicate lower concentrations of calcium. When $t = 100$, we see calcium start to diffuse across the cell as shown in Figure 3. In the following times, the confocal images show the shape of a spiral wave, that is, a spiral shaped form with center at the original location of the wave and the parts outside of the cell domain cut off.

We also show the three types of plots for $g = 50$ constant at all CRU points in Figures 4, 5, and 6. One can see that Figure 4 shows CRU opening from time to time, but no wave self-organizes, and Figure 5 shows no significant calcium cone. Figure 6 also shows no waves. We conclude from the simulations for $g = 110$ and $g = 50$ that the flux density value at which waves self-organize must lie in between these values. This motivates our choice of mean value and standard deviation when treating g as a stochastic variable in the following sections.

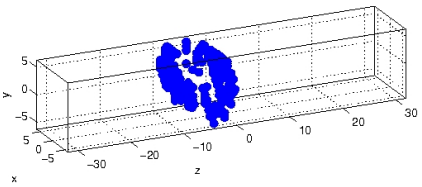

$t = 100$

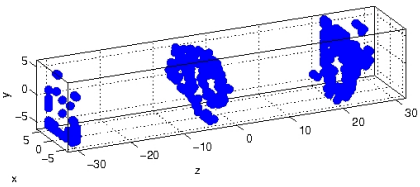

$t = 200$

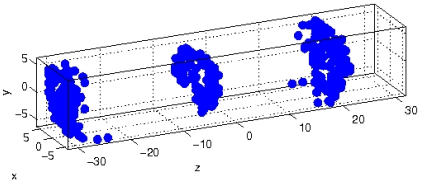

$t = 300$

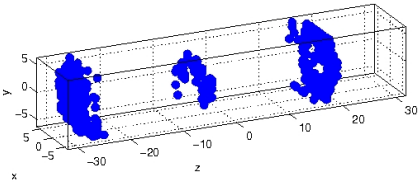

$t = 400$

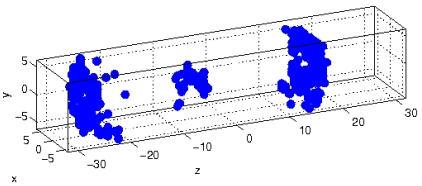

$t = 500$

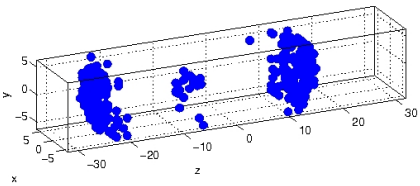

$t = 600$

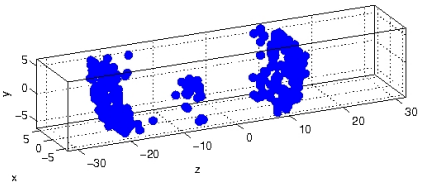

$t = 700$

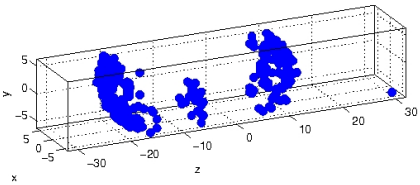

$t = 800$

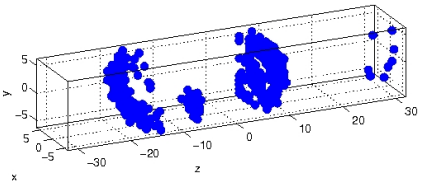

$t = 900$

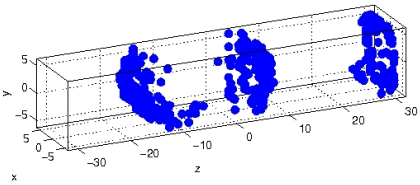

$t = 1{,}000$

Figure 1: The CRU plots for $g = 110$.

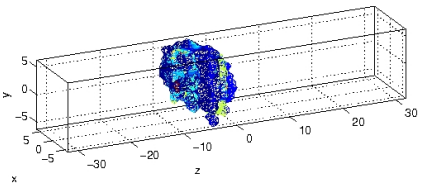

$t = 100$

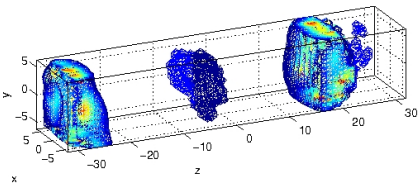

$t = 200$

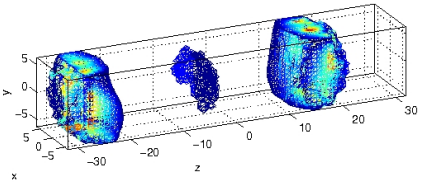

$t = 300$

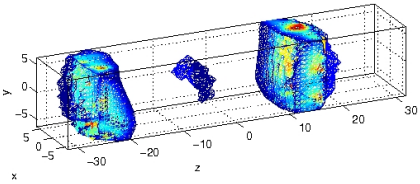

$t = 400$

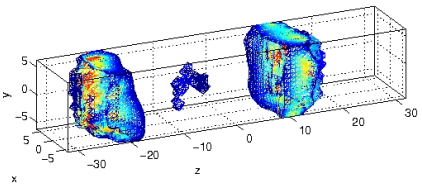

$t = 500$

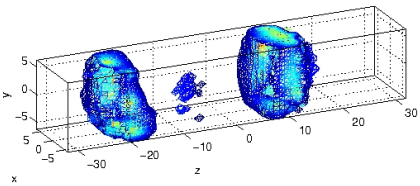

$t = 600$

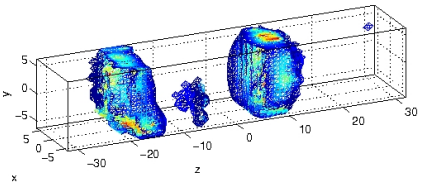

$t = 700$

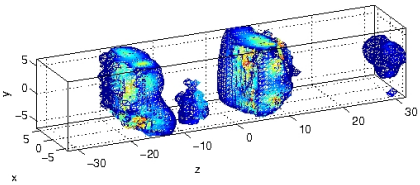

$t = 800$

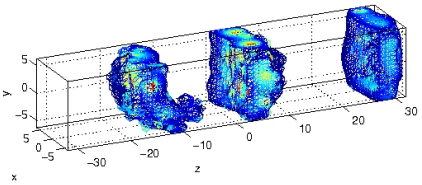

$t = 900$

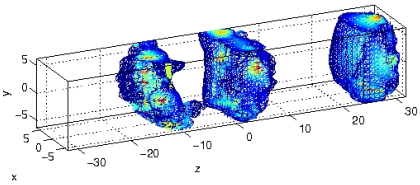

$t = 1{,}000$

Figure 2: The isosurface plots for $g = 110$.

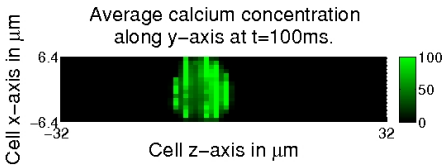

$t = 100$

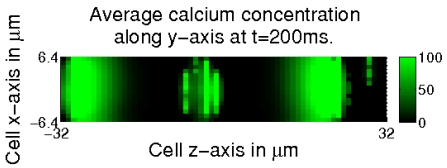

$t = 200$

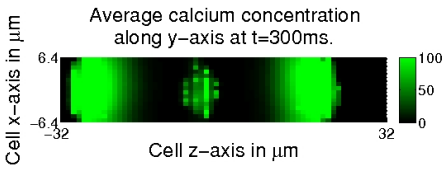

$t = 300$

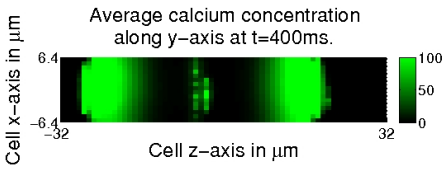

$t = 400$

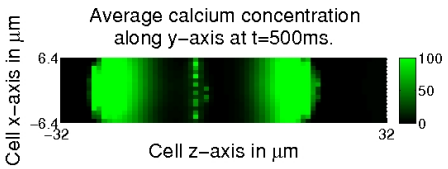

$t = 500$

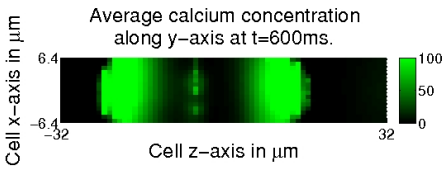

$t = 600$

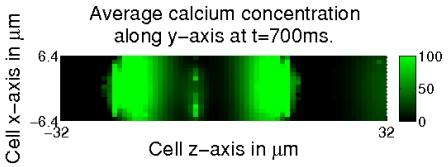

$t = 700$

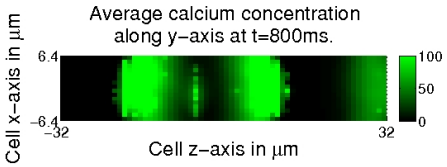

$t = 800$

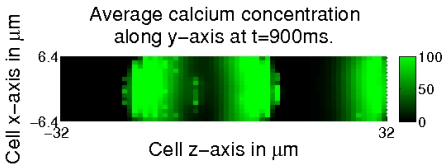

$t = 900$

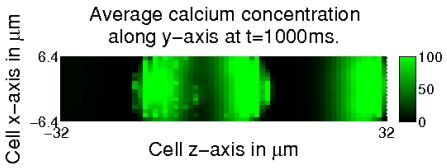

$t = 1{,}000$

Figure 3: The confocal image plots for $g = 110$.

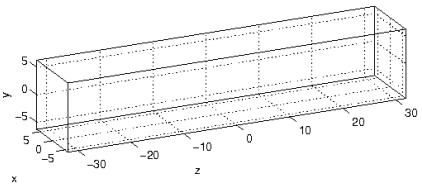

$t = 100$

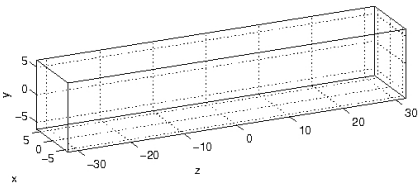

$t = 200$

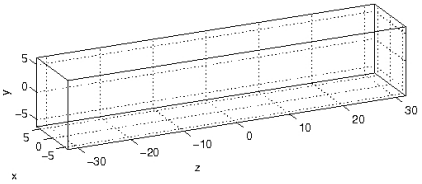

$t = 300$

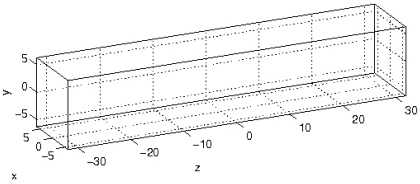

$t = 400$

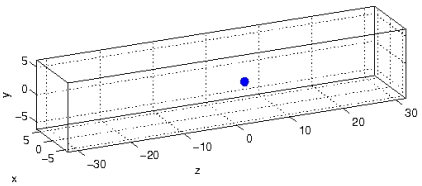

$t = 500$

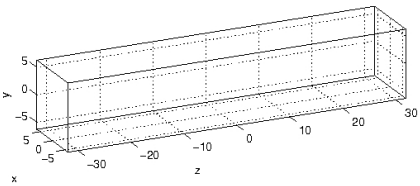

$t = 600$

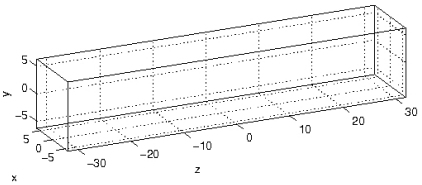

$t = 700$

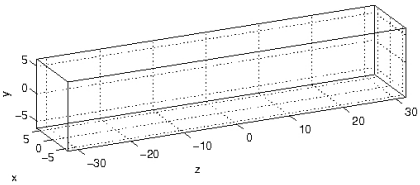

$t = 800$

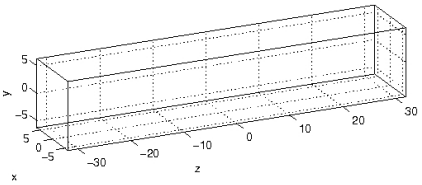

$t = 900$

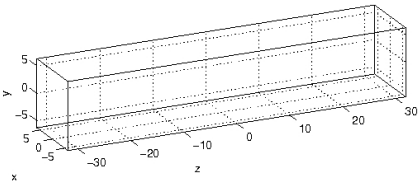

$t = 1{,}000$

Figure 4: The CRU plots for $g = 50$.

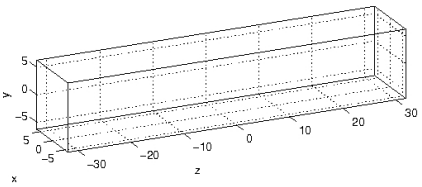

$t = 100$

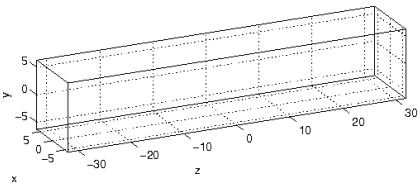

$t = 200$

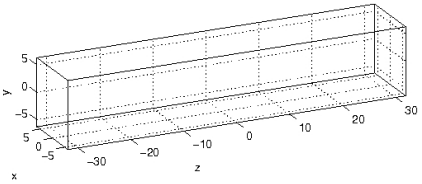

$t = 300$

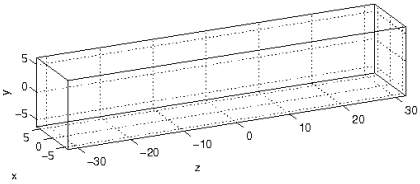

$t = 400$

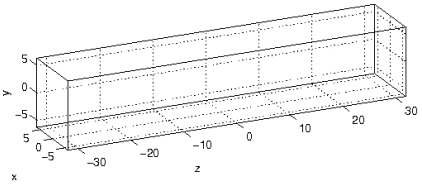

$t = 500$

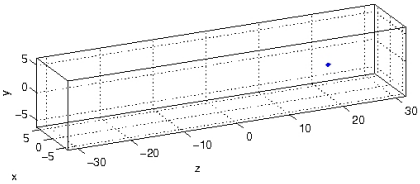

$t = 600$

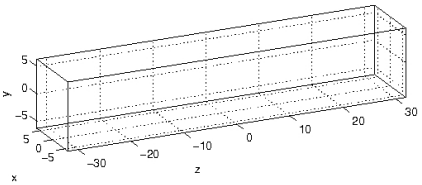

$t = 700$

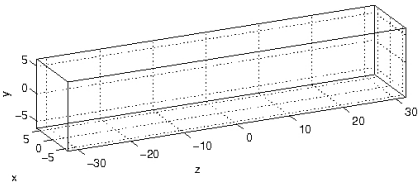

$t = 800$

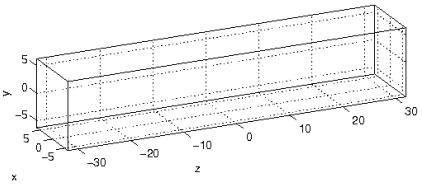

$t = 900$

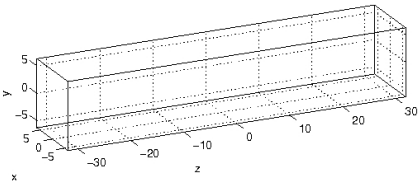

$t = 1{,}000$

Figure 5: The isosurface plots for $g = 50$.

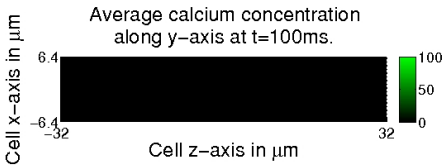

$t = 100$

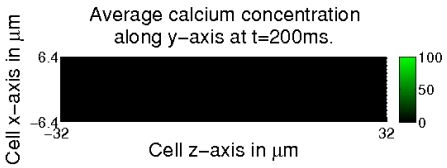

$t = 200$

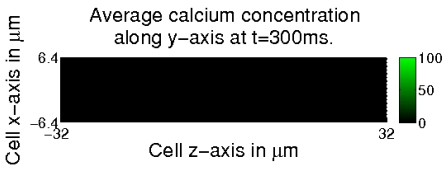

$t = 300$

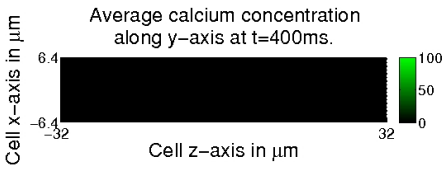

$t = 400$

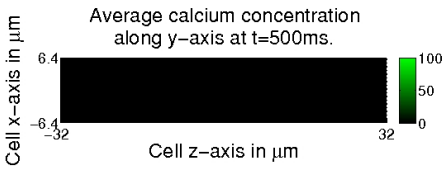

$t = 500$

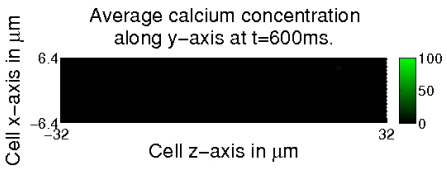

$t = 600$

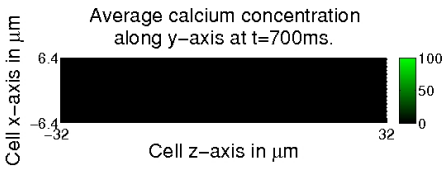

$t = 700$

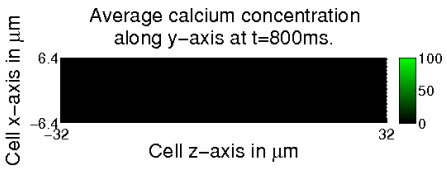

$t = 800$

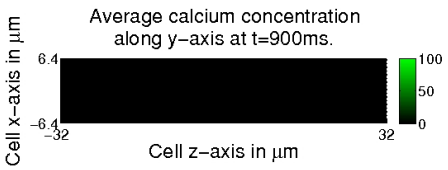

$t = 900$

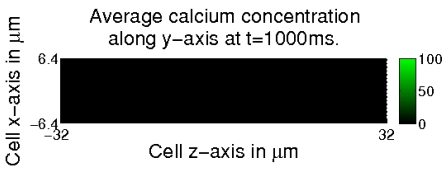

$t = 1{,}000$

Figure 6: The confocal image plots for $g = 50$.

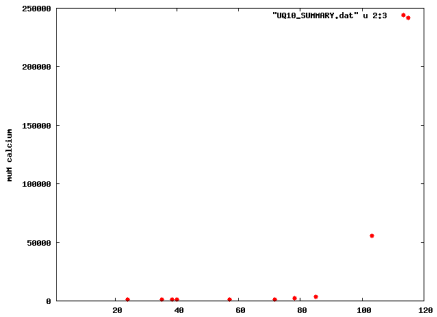

(a) M = 10 samples

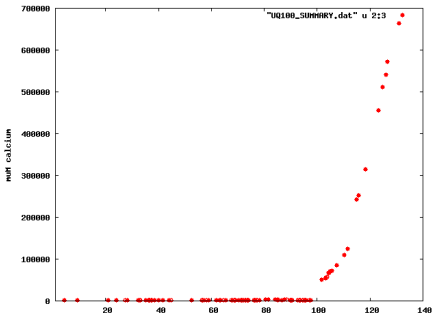

(b) M = 100 samples

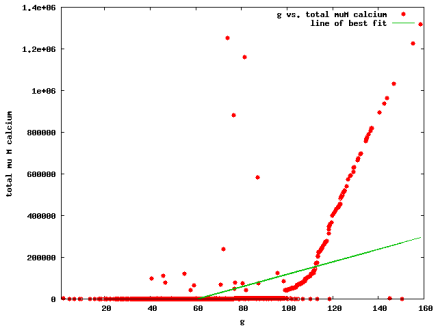

(c) M = 1000 samples

Figure 7: Plots of μ M vs. g with $t_{fin} = 100$ ms.

4.2 Spatially Uniform CRU Flux Density

4.2.1 SUCFD Simulations Using A Smaller Runtime.

We begin by analyzing the the results of the SUCFD case with $t_{fin} = 100$ ms instead of using the standard value of $t_{fin} = 1000$ ms for full simulations. We used a smaller run time to increase the speed of the simulations so that we could generate samples quickly and see if would could determine any trends from the data. The abbreviated runs take approximately less than 1 min to run as opposed to 3 to 5 minutes on average for the full simulations saving a significant amount of time as the sample size increases. The time between runs varies because the number of CRU's that are open and the amount of calcium that is released in each simulations changes with each run. The more CRU's that open the longer the code takes to run.

Figure 7 shows graphs of μM vs. total g of calcium. Figure 7 (a) was produced by compiling the data from $M = 10$ samples with g sampled from the normal distribution $N(75, 25)$ with mean of 75 μM and standard derivation 25 μM. We see that as value of g increases the total μ M of calcium also increases. Because the sample size is small we cannot predict a general trend in the data.

We increase the resolution by taking $M = 100$ samples and produce Figure 7 (b). Again we see that as the value of g increases we the total μM of calcium increases. We see a more defined trend in the data and observe that there exists some critical value of for $g \approx 100$ where the calcium concentration begins to increase.

To get a better understanding of where the critical point lies we increase the sample size yet again. Figure 7 (c) was produced by $M = 1500$ samples. We see that the previous trend in the data has continued, but a few outliers have developed. We see that critical point is more clearly defined and is slightly less than $g = 100$. To fully analyze the effects we increase the the final time to $t_fin = 1000$ and get more reliable results.

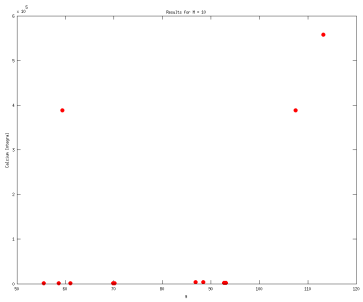

(a) M = 10 samples

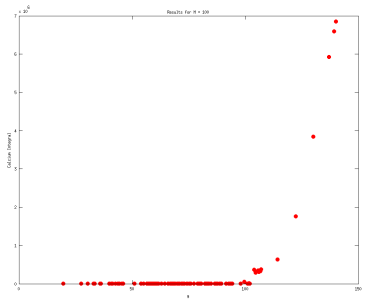

(b) = 100 samples

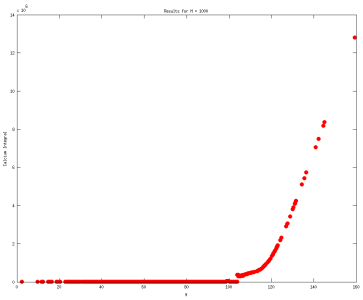

(c) M = 1000 samples

Figure 8: Plots of μ M vs. g with $t_{fin} = 1000$ ms.

4.2.2 SUCFD Simulations with $t_{fin} = 1000$ ms.

Now, we analyze the results of running the SUCFD with $t_{fin} = 1000$ ms to get a more complete picture of how g influences the behavior of the model. First, we examine the results after taking $M = 10$ samples shown in Figure 8 (a). We see that there is no noticeable trend in the data, so we increase the number of samples to $M = 100$. Figure 8 (b) shows the data for $M = 100$ samples and we see that as g increases the total amount of calcium in the cell also increases. We also see that there is a critical point at approximately $g = 100$ where calcium begins to increase dramatically. To gain a better understanding of this trend we take $M = 1000$ samples. Figure 8 shows the data for $M = 1000$ samples. We see that the trend observed with $M = 100$ samples is sustained and that as the value of g increases the total amount of calcium increases. Furthermore, we obtain a correlation coefficient of $r = 0.4553$ indicating moderate correlation.

Next, we use the data from the full simulations but scale the value calcium integral on the y axis by by the volume of the cell, $V = 10000$ so that we can better see where waves begin to self organize and propagate. Figure 9 (a) shows the results $M = 1000$ with $t_{fin} = 1000$ms with the y axis scaled by V. After scaling the y axis, we search for the critical point at which calcium integral becomes greater than 0.1μM. Figure 9 (b) shows that the critical point where activation occurs at $g \approx 71.5$ Mμm^3. In addition, we investigate the region in which the calcium integral begins to blowup. Looking at Figure 9 we see that calcium activity is occurring between $g \approx 98$ Mμm^3 and $g \approx 103$ Mμm^3. Furthermore, we see calcium begin to blowup at $g = 104$ Mμm^3.

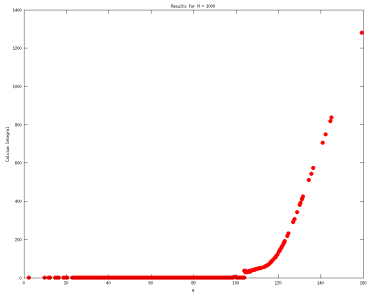

(a) M = 1000 samples with a scaled y-axis

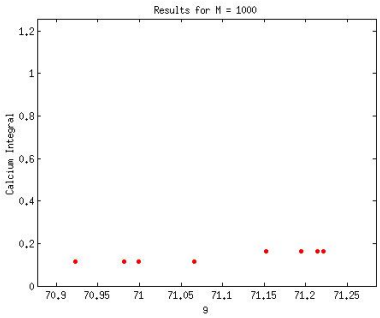

(b) Initial Region of calcium activity

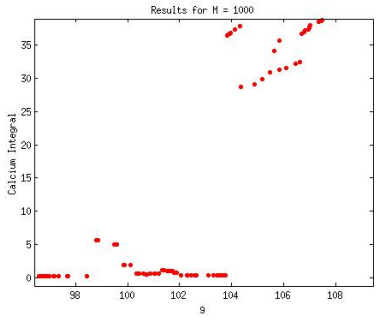

(c) Calcium blow up region

Figure 9: μ M/10000 vs. g calcium with $M = 1000$ with $t_{fin} = 1000$ ms

4.3 SICFD Simulations with $t_{fin} = 1000$ ms.

After examining the results of the SUCFD case we turn our attention to the SICFD case. To get a better understanding of how SICFD would affect the model, we design a test case. To test the effects of SICFD we let the right half of the cell have CRU values of $g_{\hat{x_r}}$ for all CRUs on that side and then we vary the left half CRU values for all CRUs on the left side $g_{\hat{x_l}}$. In our experiment we fix $g_{\hat{x_r}} = 110.0$ and we let $g_{\hat{x_l}} = 110, 105, 100, 95, 90, 85, 80, 75, 70, 65, 60, 55$.

To further illustrate how varying $g_{\hat{x_l}}$ effects the SICFD simulations we show the CRU plots for $g_{\hat{x_l}} = 110, 95, 75$, and 55 in Figures 1, 10, 11, and 12, respectively. Figure 1 shows that for $\hat{x_l} = 110$ waves form and propagate on both halves of the cell. Next, Figure 10 shows for $g_{\hat{x_l}} = 95$ that the waves on the left side of the cell begin to slow down slightly, compared to the waves on the right half. As the values $g_{\hat{x_l}}$ decrease, we see that the wave propagation on the left half eventually stops altogether around $g_{\hat{x_l}} = 55$, as illustrated in Figures 11 and 12. Therefore, these test cases illustrate how varying the value of CRUs across the cell can dramatically affect the wave velocities, possibly hindering wave propagation all together.

Finally, the linescane images in Figure 13 provide a compact summary of the behavior observed in the previous plos. The plots show how calcium concentration changes on the z-axis over time. We see that as the values of $g_{\hat{x_l}}$ decrease, the wave velocities decrease on the left side of the cell.

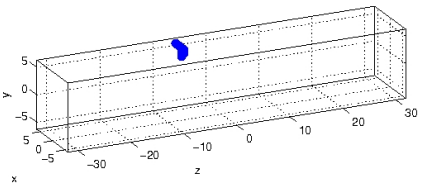

$t = 100$

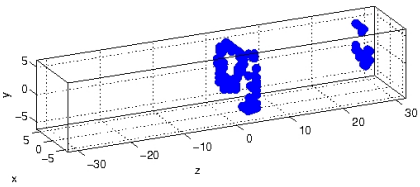

$t = 200$

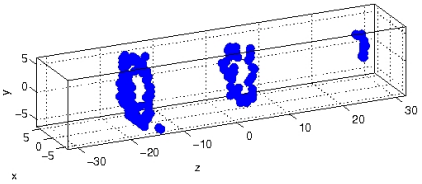

$t = 300$

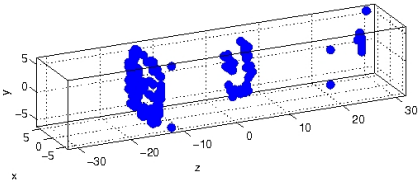

$t = 400$

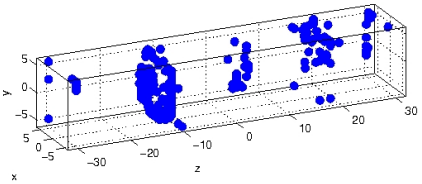

$t = 500$

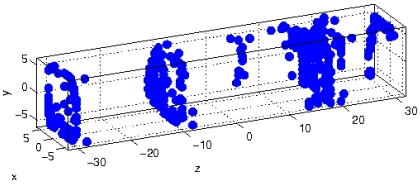

$t = 600$

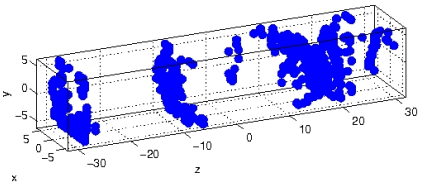

$t = 700$

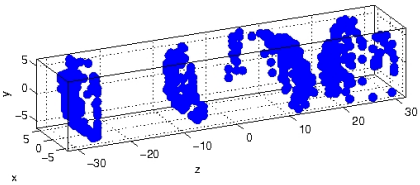

$t = 800$

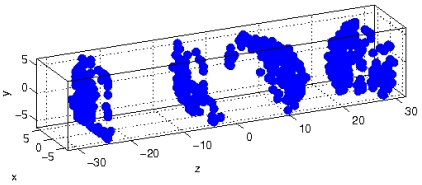

$t = 900$

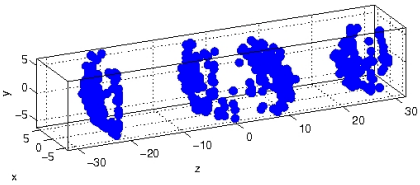

$t = 1{,}000$

Figure 10: The CRU plots with $g_{\hat{x_l}} = 95$.

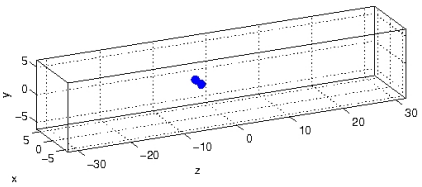

$t = 100$

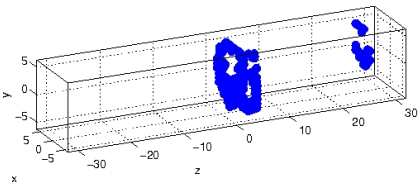

$t = 200$

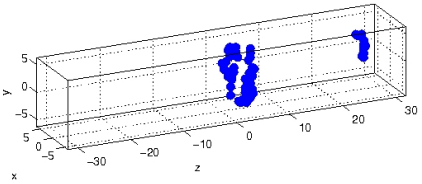

$t = 300$

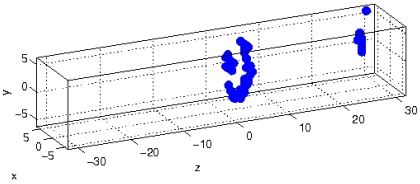

$t = 400$

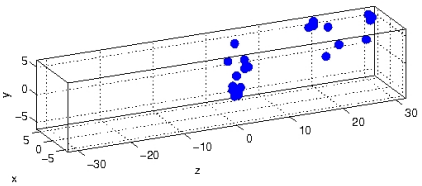

$t = 500$

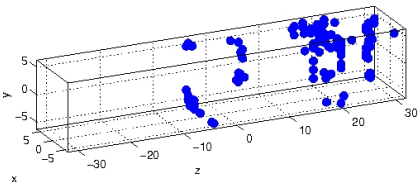

$t = 600$

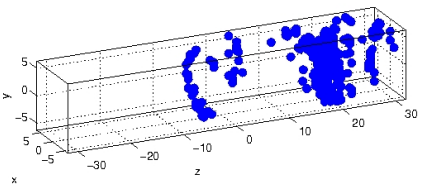

$t = 700$

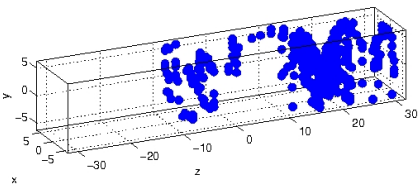

$t = 800$

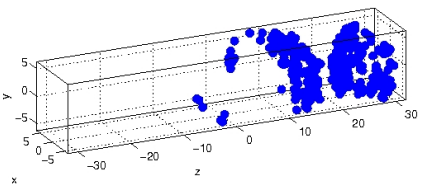

$t = 900$

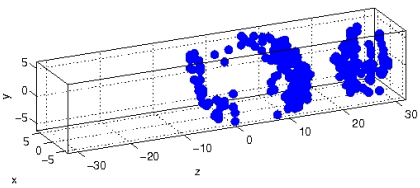

$t = 1{,}000$

Figure 11: The CRU plots with $g_{\hat{x_l}} = 75$.

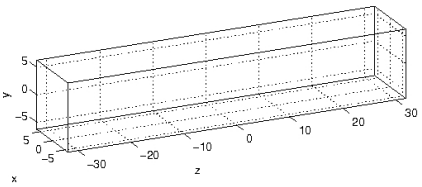

$t = 100$

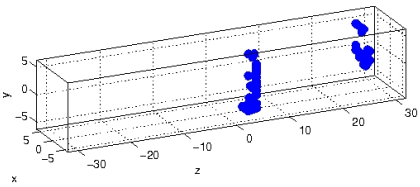

$t = 200$

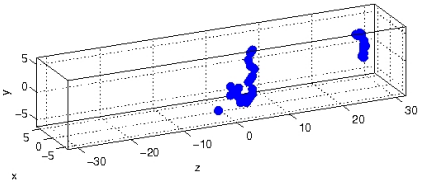

$t = 300$

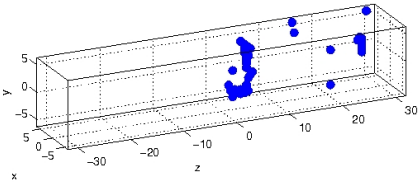

$t = 400$

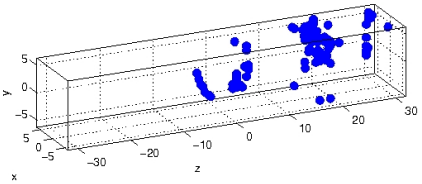

$t = 500$

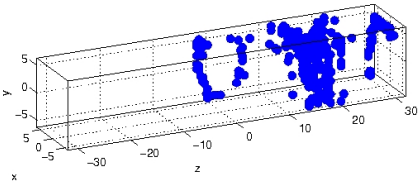

$t = 600$

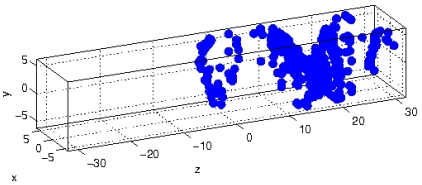

$t = 700$

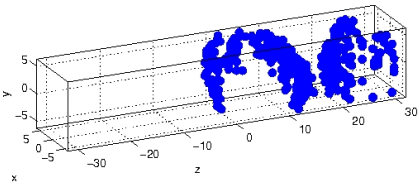

$t = 800$

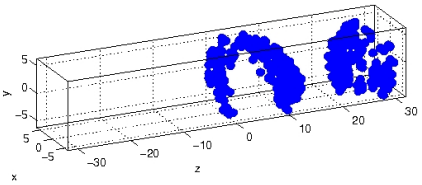

$t = 900$

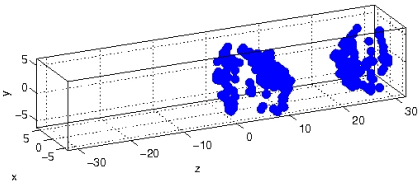

$t = 1{,}000$

Figure 12: The CRU plots with $g_{\hat{x_l}} = 55$.

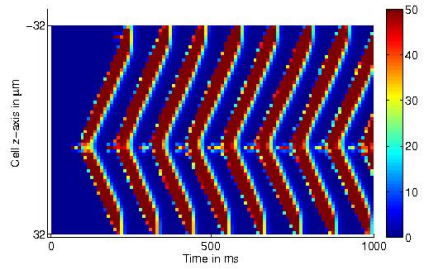

$g_{\hat{x_r}} = 110$

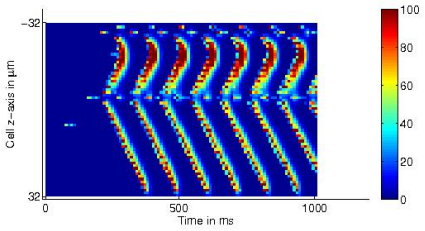

$g_{\hat{x_r}} = 100$

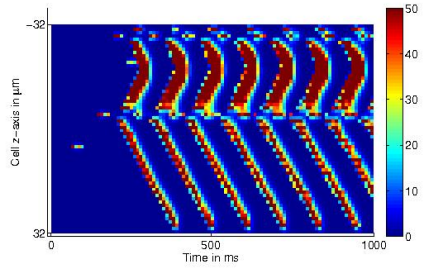

$g_{\hat{x_r}} = 90$

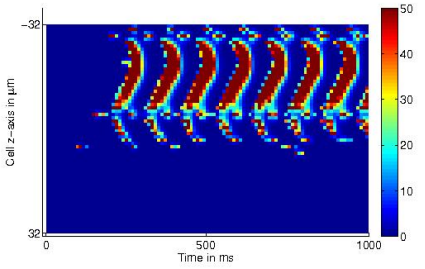

$g_{\hat{x_r}} = 80$

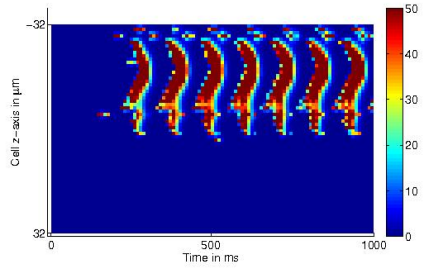

$g_{\hat{x_r}} = 70$

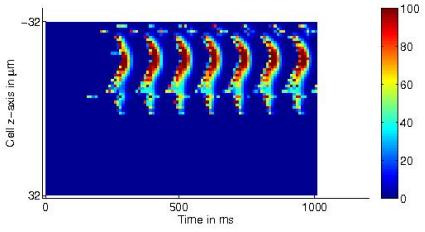

$g_{\hat{x_r}} = 60$

Figure 13: The linescan plots with $g_{\hat{x_l}} = 110, 100, 90, 80, 70, 60$.

5 CONCLUSIONS

The results of our SUCFD studies show that after a sufficient number of runs a pattern emerges in the data. We also see that shorter simulations do not represent longtime behavior because the CRUs may not have had sufficient time to open and release calcium. After running longer simulations and taking a sufficient number of samples, we can be more confident in the pattern of the data that emerges. Furthermore, we see that if the value of g is less than our critical value then it is highly unlikely that waves occur and if the value of g is greater than the critical value then it is very likely that waves will occur. Finally, more analysis of long times show that calcium activity begins near $g = 75$ which supports our choices for $\mu_g = 75$ and $\sigma_g = 25$.

Our results for the test case of the SICFD code show that the code reacts correctly to spatially non-uniform values of g. This sets the stage for fully stochastic simulations using the SICFD code.

ACKNOWLEDGMENTS

Matthew Brewster acknowledges support from the Multidisciplinary REU Program: Research, Education, and Training in Computational Mathematics and Nonlinear Dynamics of Biological, Bio-inspired and Engineering Systems at George Mason University (GMU) in the Summer of 2013. Furthermore, the author would like to thank Dr. Matthias K. Gobbert at UMBC (`gobbert@umbc.edu`) and Dr. Padmanabhan Seshaiyer at GMU for providing the research opportunity, guidance, and support. In addition, the author would like to thank the graduate students, Xuan Huang, Samuel Khuvis, Zana Coulibaly, and Jonathan Graf for their help in implementing the code, and their insights. The hardware used in the computational studies is part of the UMBC High Performance Computing Facility (HPCF). The facility is supported by the U.S. National Science Foundation through the MRI program (grant nos. CNS–0821258 and CNS–1228778) and the SCREMS program (grant no. DMS–0821311), with additional substantial support from the University of Maryland, Baltimore County (UMBC).

REFERENCES

[1] Matthew Brewster, Maziar Raissi, Padmanabhan Seshaiyer, and Timothy Sauer. A parallel infrastructure for solving differential equations with random inputs and Monte Carlo simulations for big data. Technical report, George Mason University, 2013.

[2] Zana Coulibaly, Michael Muscedere, Matthias K. Gobbert, and Bradford E. Peercy. Long-time simulation of calcium waves in a heart cell to study the effects of calcium release flux density and of coefficients in the pump and leak mechanisms on self-organizing wave behavior. Technical Report HPCF–2009–6, UMBC High Performance Computing Facility, University of Maryland, Baltimore County, 2009.

[3] Zana A. Coulibaly, Bradford E. Peercy, and Matthias K. Gobbert. Insight into spontaneous recurrent calcium waves in a 3-D cardiac cell based on analysis of a 1-D deterministic model. Published online (2014).

[4] Matthias K. Gobbert. Long-time simulations on high resolution meshes to model calcium waves in a heart cell. *SIAM J. Sci. Comput.*, vol. 30, no. 6, pp. 2922–2947, 2008.

[5] James P. Keener. Stochastic calcium oscillations. *Math. Med. Biol.*, vol. 23, no. 1, pp. 1–25, 2006.

[6] Jonas Schäfer, Xuan Huang, Stefan Kopecz, Philipp Birken, Matthias K. Gobbert, and Andreas Meister. A memory-efficient finite volume method for advection-diffusion-reaction systems with non-smooth sources. Published online (2014).